Semiconductor Physics, Quantum Electronics & Optoelectronics, 2026. V. 29, No 2. P. 180-190.

Hetero- and low-dimensional structures

Tunable emission of indotetracarbocyanine dyes due to solvate variation and interaction with carbon nanotubes

A.B. Verbitsky[1], Yu.P. Piryatinski[1], O.D. Kachkovskyy[2], O.V. Yatsun[3], K.O. Maiko[4], A.G. Rozhin[5], P.M. Lutsyk[5,*]

[1]*Institute of Physics, National Academy of Sciences of Ukraine, 46 Nauky Avenue, 03680 Kyiv, Ukraine*
[2]*Institute of Bioorganic Chemistry and Petrochemistry, National Academy of Sciences of Ukraine, 1 Murmanska Street, 02660 Kyiv, Ukraine*
[3]*National University of Life Resources and Environmental Management of Ukraine, 12 Heroiv Oborony Street, 03041 Kyiv, Ukraine*
[4]*Faculty of Radio Physics, Electronics and Computer Systems, National Taras Shevchenko University of Kyiv, 4 Hlushkova Avenue, 03127 Kyiv, Ukraine*
[5]*Aston Institute of Photonic Technologies, School of Engineering and Innovation, Aston University, Aston Triangle, B4 7ET, Birmingham, UK*
[*]*Corresponding author e-mail: p.lutsyk@aston.ac.uk*

Abstract. Indotetracarbocyanines belong to a family of long cyanine dyes that easily change molecular shape from symmetric cyanine-like to asymmetric polyene state. Multiple factors affect the conformations of such molecules and therefore influence their photoluminescent emission. In this paper, we investigated the photophysical behavior of indotetracarbocyanine dyes in various solvent environments and in mixtures with single-walled carbon nanotubes. The results revealed concentration-, aging-, and solvent-polarity dependent spectral features of such dyes, allowing us to establish key mechanisms for emission tuning. The spectral changes have been associated with symmetry-dependent molecular conformations of indotetracarbocyanines and their ability to interact with carbon nanotube surfaces. New emission bands emerge in the photoluminescence spectra due to dye-nanotube interactions, mediated by π–π stacking and electrostatic effects. This behavior is consistent with adsorption-induced aggregation of the dye on the nanotube surface and with the formation of new photoinduced emitting states.

Keywords: cyanine dyes, carbon nanotubes, photoluminescence, fluorescence, cyanine and polyene states, solution aging.

https://doi.org/10.15407/spqeo29.02.180
PACS 33.50.Dq, 61.25.H-, 61.48.De, 78.55.Kz

Manuscript received 03.04.26; revised version received 28.05.26; accepted for publication 10.06.26; published online 23.06.26.

1. Introduction

Cyanine dyes are of widespread scientific interest owing to their delocalized π-electron systems, strong tunable absorption from visible to the near-IR region, and high photoluminescence (PL) efficiency [1–8]. These dyes exhibit pronounced sensitivity to local polarity, molecular packing, and aggregation state, making them highly effective probes for investigating interfacial interactions and exciton dynamics in hybrid nanostructures. They are well-suited for functionalization of carbon nanotubes (CNT) [9–12]. CNTs are one-dimensional nanostructures that exhibit exceptional electrical, optical, and mechanical properties, enabling their application across a broad range of fields, from high-performance composite materials to biosensing and near-IR photonics [11–14]. A critical requirement for these applications is the functionalization of nanotubes with organic molecules, modulating the photophysical properties of nanotubes through non-covalent interactions, such as π–π stacking and charge transfer. Previous studies have shown that cyanine dyes can sensitize CNT emission or activate higher-energy emissive states upon complex formation [9–12]. The interaction of the dye molecules with the nanotubes, as well as the aggregation behavior of the dyes on the nanotube surface, is strongly governed by the conformational state of the dye [12].

The electronic structure of a cationic polymethine dye can be described in terms of three limiting configurations [6]: (A) a symmetric cyanine state, in which the positive charge is fully delocalized along the conjugated chain; (B) an asymmetric dipolar state, characterized by

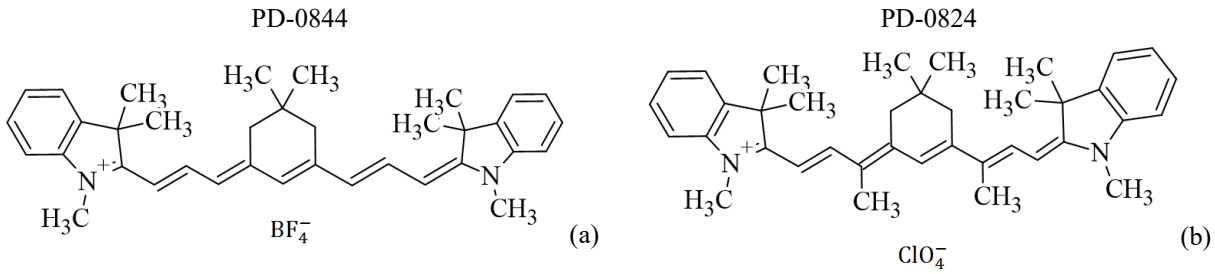

Fig. 1. The chemical formulas of indotetracarbocyanine dyes PD-0844 (a) and PD-0824 (b).

charge localization on one of the terminal groups; and (C) a bis-dipolar state, in which the charge is concentrated at the central atom of the conjugated chain/bridge. The electronic configuration adopted by the dye is governed by both intrinsic molecular parameters (the length of the π-conjugated chain, the donor strength of the terminal substituents, and the degree of bond-length equalization) and external environmental factors, including solvent polarity, counterion identity, and temperature. For example, a polar environment or specific counterion coordination can induce symmetry breaking and shift the equilibrium toward the asymmetric (B) configuration already in the electronic ground state [7, 8]. In the limiting cases, symmetric (A) and asymmetric (B) charge localizations along the π-conjugated backbone render the electronic structure of the dyes analogous to cyanine-like and polyene-like systems, respectively. For dyes with extended polymethine chains absorbing in the red and near-IR spectral regions, the symmetric, bond-equalized configuration becomes energetically unstable. This instability gives rise to Peiperl's distortion and the formation of localized dipolar charge distributions [7]. As a result, strong parallels can be drawn between polymethine dyes and polyenes or polysubstituted polyacetylenes, where analogous bond alternation effects lead to distinct optical transitions. Most cationic polymethine dyes are close to the ideal cyanine state, where the positive charge is evenly delocalized between terminal donor groups through the conjugated bridge. This state is characterized by bond-length equalization and manifests as narrowband ("solitonic") absorption [6] accompanied by intense PL. Such spectral features reflect the formation of topological excitations, analogous to soliton states in conducting polyenes, highlighting potential connections to topological phenomena in organic photonics. Thus, the three-configuration model rationalizes the optical properties of the dyes and relates their behavior to extended conjugated systems exhibiting Peiperl's distortion, soliton excitations, and polaron dynamics. This perspective positions polymethine dyes as unique molecular systems for probing charge delocalization and as promising candidates for dye lasers, nonlinear optics, and biofluorescent probes.

However, indotetracarbocyanine dyes featuring a long carbon chain tend to easily break symmetry, which strongly impacts their spectral features. Furthermore, strong coupling of π-electrons to vibrational modes and solvation fields leads to large-radius polaronic states, which significantly influence relaxation dynamics and spectral shifts in such systems. In this work, we investigated absorption and PL behavior of indotetracarbocyanine dyes in both neat solutions and dye-CNT mixtures, emphasizing the impact of solvent polarity and solution aging, to elucidate how long-chain indotetracarbocyanine dyes change their optical properties in a variable solvate environment and π–π interactions with CNTs.

2. Experimental details

2.1. Sample preparation

Studied indotetracarbocyanine dyes: PD-0844 with BF_4^- counterion and PD-0824 with ClO_4^- counterion (Fig. 1) were dissolved in non-polar (toluene) and polar (acetonitrile, dimethylformamide (DMF), N-methyl-2-pyrrolidone (NMP)) solvents. The dyes were supplied by the Institute of Organic Chemistry (NASU, Ukraine). The dye purity was determined using NMR as well as liquid chromatography and mass spectrometry (LC-MS) and found to be approx. 95%. The following dye concentrations were studied: 0.004, 0.02, 0.1, and 0.2 mg/mL.

Purified single-wall CNTs (CoMoCAT) were purchased from SWeNT, Inc. (SWeNT CG100, Lot # 000-0012) and used as a source material to prepare dispersions of nanotubes. CNT powder (1.6 mg) was dispersed in NMP (10 mL) by bath ultrasonication (NanoRuptor, Diagenode) for 1 h at 21 kHz and 250 W. After ultrasonication, the dispersions were ultracentrifuged at 47 000 rpm for 2 h 30 min at 17 °C (Beckman Coulter Optima Max-XP, MLS 50 rotor) to remove the CNT aggregates and obtain supernatant with debundled CNTs. Such supernatant dispersions of CNT were used to prepare mixtures with NMP solutions of the studied dyes in a proportion of 1:1.

2.2. Experimental setup

The absorption spectra within the visible and NIR ranges were measured using a Lambda 1050 UV/VIS/NIR (Perkin Elmer) spectrometer. The PL emission spectra at various excitation wavelengths were recorded using a Horiba NanoLog excitation–emission spectrofluorometer equipped with a nitrogen-cooled InGaAs array detector to generate PL excitation-emission maps (PLE maps), with the X-axis representing the wavelength of the PL emission, λ_{em}, and the Y-axis representing the excitation

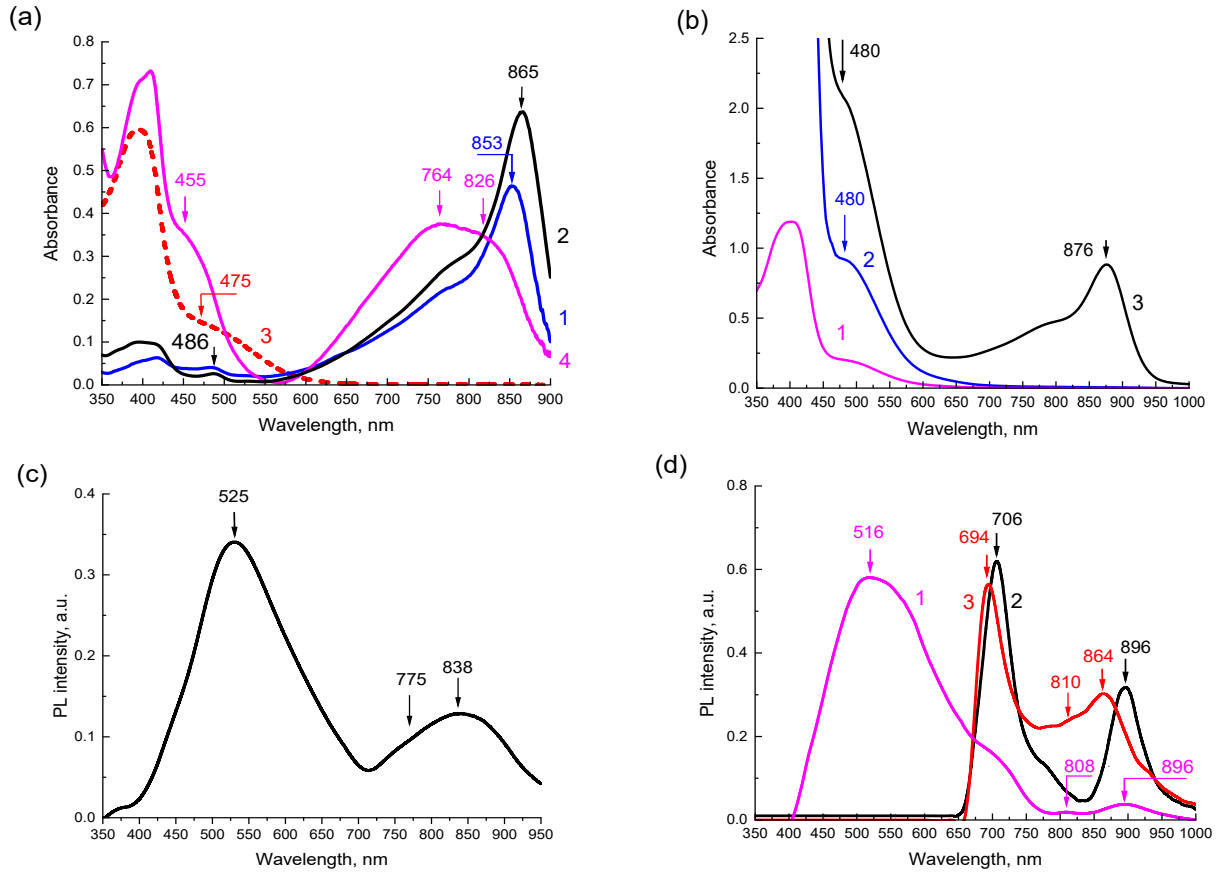

Fig. 2. (a) Absorbance spectra of PD-0824 dye at the concentration 0.01 mg/mL in acetonitrile (*1*), DMF (*2*, *3*), and toluene (*4*) solutions; the solutions are freshly prepared (*1*, *2*, *4*) and aged for 24 hours (*3*). (b) Absorbance spectra of a fresh solution of PD-0844 dye in NMP of various concentrations: 0.02 (*1*), 0.1 (*2*), and 0.2 (*3*) mg/mL. (c) PL spectrum of PD-0824 dye at the concentration 0.01 mg/mL in toluene; λ_{ex} = 385 nm (*2*). (d) PL spectra of PD-0824 dye in DMF at the concentration 0.01 (*1*, *2*) and 0.2 mg/mL (*3*); the solutions are freshly prepared (*1*, *2*) and aged for 24 hours (3); λ_{ex} = 385 nm (*1*) and 620 nm (*2*, *3*).

wavelength, λ_{ex}. Entrance/exit slits (bandpass) of 14 nm in width were used for both the excitation and emission monochromators in the NIR PL measurements. The PL experiments within the visible range were performed using a silicon detector and 2 nm entrance/exit slits (bandpass) for the monochromators. All measurements were done at room temperature (T = 296 K).

2.3. Quantum-chemical modelling

Gaussian 16 was used for the quantum-chemical calculations, which were performed at the DFT/CAM-B3LYP/6-311++G(d,p) level of theory [15]. The CAM-B3LYP functional is widely used for extended π-conjugated systems, as it provides molecular geometries close to experimentally observed structures and improves the accuracy of excitation energies for the Rydberg and charge-transfer states [16, 17]. Geometry optimization and frequency calculations in the gas phase were carried out for the molecular structure. As a result, the dihedral angle (C–C–C–N) between one of the indole terminal groups and the conjugated chain was found to be approximately +179°, and this part of the molecule can therefore be considered nearly planar. Dihedral angle between second terminal group (C–C–C–N) is approximately 179°; therefore, the side profile of the molecules, formed by the conjugated chain and the terminal groups, is slightly bent.

3. Results and discussion

3.1. Absorption spectra and quantum chemical modeling of neat solutions of the dyes

In polar solvents, the absorption spectra of the dyes exhibit a strong dependence on both dye concentration and the time elapsed after solution preparation. Freshly prepared molecular solutions of the dyes in acetonitrile (Fig. 2a, curve *1*) and DMF (Fig. 2a, curve *2*) display spectral features characteristic of symmetric cyanine dyes, with long-wavelength absorption maxima at 853 and 856 nm, respectively. Higher-energy $S_0 \rightarrow S_n$ transitions at wavelengths below 530 nm are only weakly expressed. Notably, the time-dependent evolution (aging) of the absorption spectra of the studied dyes in polar solvents also depends on the atomic structure of the solvent's polar functional groups. Thus, despite the comparable polarity of acetonitrile, DMF, and NMP,

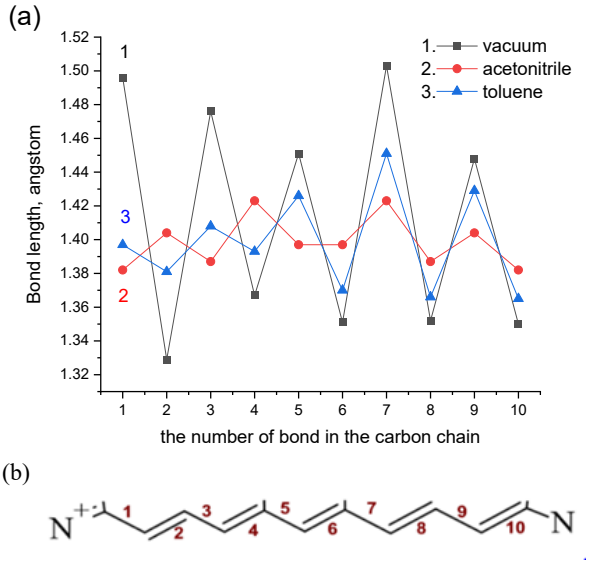

Fig. 3. (a) Calculated bond lengths in conjugated carbon chain of the studied dyes after optimization in vacuum (*1*), acetonitrile (*2*), toluene (*3*) in the ground state *versus* the number of bonds in the conjugated carbon chain as shown in (b).

acetonitrile solutions of the dyes show almost no spectral changes over time. In contrast, solutions of the dyes in DMF and NMP undergo pronounced spectral transformations with the absorption spectra becoming increasingly dominated by higher-energy $S_0 \rightarrow S_n$ bands appearing at wavelengths below 570 nm. For example, in DMA solutions, a pronounced absorption band emerges at ~ 400 nm, accompanied by a shoulder near 500 nm (Fig. 2a, curve *3*), which can be assigned to the $S_0 \rightarrow S_2$ transition.

In addition to the aging effect above, dye concentration affects the absorption spectra in DMF and NMP, *e.g.*, the absorption spectra of the studied dyes in polar NMP exhibit a strong dependence on both the time elapsed after solution preparation and the dye concentration. In freshly prepared low-concentration solutions of PD-0844 in NMP (Fig. 2b, curves *1*, *2*), absorption is observed predominantly in the higher-energy $S_0 \rightarrow S_n$, with minimal contribution from the $S_0 \rightarrow S_1$ transition. With increasing concentration, a new band appears at 876 nm (Fig. 2b, curve *3*) in the $S_0 \rightarrow S_1$ region, reflecting planarization and restricted conformational flexibility of the molecules at close intermolecular distances.

The absorption of the studied dyes in nonpolar toluene does not change significantly over time. Absorption spectrum of indotetracarbocyanine molecules exhibits a decrease in the intensity of the electronic 0–0 transition, accompanied by enhanced first vibronic 0–1 band associated with the symmetric dye conformation, with bands at 826 and 764 nm (Fig. 2a, curve *4*). In the higher-energy $S_0 \rightarrow S_n$ region, a substantial increase in the intensity of the absorption bands at 455 and 400 nm is detected, indicating enhanced population of these excited states.

Bond lengths (in the ground state) for the conjugated carbon chain of the studied indotetracarbocyanines have been calculated in polar and non-polar solvent environments, as shown in Fig. 3. Changes in the bond lengths of the carbon chain demonstrate that polar solvents (*e.g.*, acetonitrile, *etc.*) stabilize bond lengths, where molecular conformations are symmetrical to the center of the chain (Fig. 3, curve *2*). For the dye molecules in non-polar toluene, drastic changes in bond lengths can be observed (Fig. 3, curve *3*). This result correlates with the absorption spectra observed in polar and non-polar environments for freshly prepared solutions of the dye.

These observations highlight the critical role of the solvent in modulating the electronic structure and optical response of indotetracarbocyanines, revealing a strong interplay between molecular symmetry, charge localization, and solvent polarity [18, 19]. In both nonpolar (toluene) and polar solvents (DMF, NMP), the dyes behave as asymmetric dipoles with preferential localization of the positive charge at one terminal group. Polar solvents, as well as specific counterion coordination, can induce symmetry-breaking already in the electronic ground state. The relaxation pathways of electronic excitation in such polymethine systems can be analyzed using the Frenkel exciton model [20], which provides a robust theoretical basis for describing the dynamics of the initially excited states.

During the initial stages of solvation (fresh solution), the studied dyes remain predominantly in the symmetric cyanine state, thereby allowing efficient $S_0 \rightarrow S_1$ absorption. As solvation proceeds (aging solution), the asymmetric conformation becomes progressively stabilized, resulting in enhanced $S_0 \rightarrow S_2$ absorption within the near-UV range. One- and two-photon spectroscopic studies of related dyes [19] assign the absorption band at 862 nm to the $S_0 \rightarrow S_1$ transition of the symmetric form, whereas the intense band at 520 nm and the weaker band near 740 nm are attributed to the asymmetric conformations possessing a spontaneous dipole moment. Accordingly, the absorption bands observed within 480…500 nm and 760…780 nm ranges can be assigned to the $S_0 \rightarrow S_2$ and $S_0 \rightarrow S_1$ transitions of the asymmetric conformation, respectively. The redistribution of absorption bands in the $S_0 \rightarrow S_1$ and $S_0 \rightarrow S_2$ spectral ranges is driven by both the polarity and the atomic structure of the solvent's polar functional groups. This behavior is fully consistent with the ground-state model [21, 22], which is widely applied to polymethine dyes to explain symmetry breaking and two-photon absorption characteristics [19]. In weakly polar media [23], dye molecules retain a symmetric distribution of charge along the polymethine chain, corresponding to the cyanine state. In contrast, the strong electric field of highly polar solvents disrupts this symmetry, inducing asymmetric charge localization toward one terminal group and promoting a transition to a polyene-like asymmetric conformation.

NMP and DMF are highly polar aprotic solvents that strongly solvate cationic salts of the studied dyes through charge–dipole interactions between positively charged dye terminals and negatively polarized oxygen atoms of the solvent molecules. This coordination results

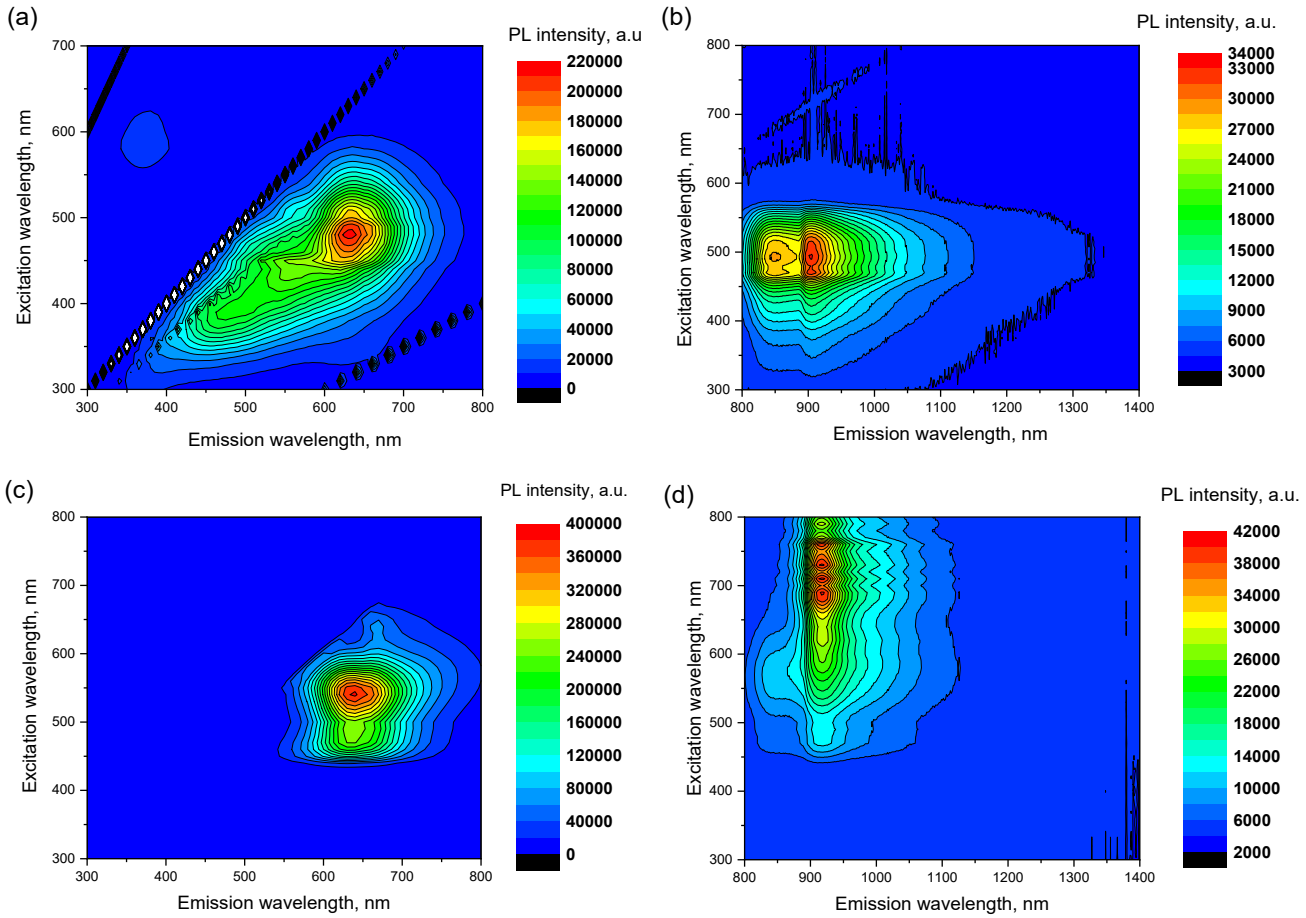

Fig. 4. PLE maps of fresh solutions of PD-0844 in NMP solvent for low (a, b – 0.02 mg/mL) and high (c, d – 0.2 mg/mL) dye concentrations.

in the formation of stable solvation shells around the terminal groups of the dyes, effectively isolating them from the π-conjugated carbon chain and thereby altering intramolecular charge redistribution upon optical excitation. Comparative experiments show that while solutions of the studied dyes in acetonitrile retain their optical properties for weeks with only minor perturbations of molecular symmetry, the same dyes in NMP and DMF exhibit rapid spectral changes within hours, consistent with strong disruption of symmetry. Such behavior is attributed to the more pronounced solvation of terminal groups in NMP and DMF compared to acetonitrile.

Naturally, one alternative explanation is also the decomposition of the molecule. But since in some solvents the spectra remain unchanged (see above), we consider that most probably the formation of an asymmetric form and aggregation occurs.

3.2. PL spectra and PLE maps for dye solutions

Fig. 2c presents the PL spectra of PD-0824 molecular solutions in toluene. The PL spectra are dominated by intense emission from the S_2 excited state, with a pronounced emission band centered at 525 nm, accompanied by a weak PL in the $S_0 \rightarrow S_1$ region, observed as emission bands at 775 and 838 nm. Observed PL features of indotetracarbocyanines in non-polar toluene are consistent with the explanation of the absorption spectra above (Fig. 2a).

For a freshly prepared molecular solution of studied dyes in the polar DMF, both the spectral distribution and the relative intensities of the PL bands exhibit a strong dependence on the excitation wavelength (λ_{ex}). Excitation at higher photon energies, above the $S_0 \rightarrow S_2$ transition (λ_{ex} = 385 nm), leads to an intense emission from the S_2 state, manifested as a prominent band at 516 nm (Fig. 2d, curve *1*). This emission is accompanied by weaker S_1 bands at 864 and 896 nm, as well as by an additional spectral feature at 706 nm, located between the S_1 and S_2 emission regions. When λ_{ex} is tuned below the $S_0 \rightarrow S_2$ transition (λ_{ex} = 620 nm), the PL spectrum is dominated by S_1 emission peaking at 896 nm; nevertheless, the 706 nm band remains (Fig. 2d, curve *2*). The persistence of this feature at different excitation conditions suggests the involvement of intermediate electronic states, commonly referred to as "dark states," due to breaking and charge-transfer interactions in polar environments.

With increasing time after solution preparation (solution aging), the PL spectra in DMF undergo significant changes (Fig. 2d, curve *3*). In particular, the 864 nm band becomes more pronounced and can be

assigned to the radiative $S_1 \rightarrow S_0$ transition, indicating relaxation toward a stabilized lowest excited-state configuration. The evolution of the spectral profile, together with the consistent presence of the 706 nm band, supports the involvement of photoinduced intramolecular charge-transfer (ICT) states. These states are favored in highly polar environments and can mediate efficient nonradiative relaxation channels, while simultaneously reshaping the balance between S_1 and S_2 emission [23].

In addition to the aging effect, dye concentration impacts the PL spectra of the dyes. Fig. 4 shows PLE maps of freshly prepared solutions of PD-0844 in NMP at low (Figs. 4a, 4b – 0.02 mg/mL) and high (Figs. 4c, 4d – 0.2 mg/mL) concentrations of the dye. The PLE maps demonstrate that, at both concentrations, the spectral distribution and overall PL intensity strongly depend on λ_{ex}. PL from higher excited states, with a maximum of 640 nm observed at low and high concentrations of the dye (Figs. 4a, 4c). For the 0.02 mg/mL solution, PL is observed within 470…650 upon excitation between 400 and 550 nm. In contrast, the 0.2 mg/mL solution exhibits PL within 600…700 at excitation from 450 to 550 nm, suggesting concentration-dependent spectral behavior likely related to aggregation effects. PL from the states above S_1 is generally suppressed by ultrafast internal conversion, yet indotetracarbocyanines exhibit pronounced anti-Kasha emission upon excitation of higher $S_0 \rightarrow S_n$ ($n > 1$) states. This behavior can be rationalized by the combination of large $S_2 - S_1$ energy gaps (0.6…1.0 eV) and strong $S_0 \rightarrow S_2$ oscillator strengths, which reduce internal conversion rates and enable radiative transitions from upper states [24].

In diluted solutions (0.02 mg/mL), emission from the S_1 state is observed only when molecules are excited *via* higher electronic states (spectral window 470…530 nm); direct excitation of the S_2 transition does not produce a detectable S_1 emission (Fig. 4b). In the $S_1 \rightarrow S_0$ spectral range of these diluted solutions two bands of comparable intensity are resolved at 850 and 907 nm. We can associate the shorter-wavelength component (850 nm) with emission from species with broken molecular symmetry, and the longer-wavelength component (907 nm) with emission from more symmetric molecular configurations. At high concentration of the dye (0.2 mg/mL), the spectral pattern changes significantly: emission from the S_1 becomes observable even upon excitation below the S_2 band (Fig. 4d). The PL excitation spectrum shows distinct features within 680…790 nm, and the $S_1 \rightarrow S_0$ PL maximum is dominated by emission from the symmetric molecular population – shifts further to the red up to 918 nm (Fig. 4d).

These concentration-dependent observations indicate that the increase in the symmetric-molecule contribution with concentration is not solely a consequence of solvent solvation but depends critically on intermolecular interactions. At higher concentrations, the dye molecules are likely to experience stronger π–π and dipole–dipole contacts that (i) promote a more planar geometry, (ii) enhance electronic delocalization along the polymethine chain, and (iii) allow partial exciton delocalization or coupling between nearby chromophores. Together, these effects stabilize symmetric (delocalized) electronic configurations and increase their radiative yield, producing both the enhanced intensity of the longer-wavelength band and the observed red shift of the $S_1 \rightarrow S_0$ maximum. In summary, the PLE maps demonstrate a pronounced, concentration-dependent shift of the studied dyes toward symmetry-preserving, delocalized electronic states in polar NMP; this shift is driven by a combination of efficient solvation of the cationic chromophore and concentration-induced intermolecular interactions that tend to planarize and electronically couple neighboring molecules.

Observed spectral behavior is consistent with a symmetry-breaking scenario, where the initially symmetric cyanine-like charge distribution of the polymethine chain is destabilized by the strong electric field of the polar solvent. This process induces a transition from the symmetric “cyanine” state to the asymmetric “polyene” state, accompanied by a redistribution of oscillator strength from the $S_0 \rightarrow S_1$ transition into higher-energy bands. As time progresses and solvent–solute interactions become fully established, the stabilization of the asymmetric charge-transfer conformation leads to the emergence of intense absorption bands within the near-UV and visible ranges, particularly associated with the $S_0 \rightarrow S_2$ transition.

These observations agree with the essential-state model [21, 22], which successfully explains solvent- and symmetry-induced spectral transformations in polymethine dyes. Furthermore, the time-dependent evolution of the spectra in NMP highlights the role of intermediate “dark states” and ICT configurations [23]. Thus, our studies clearly demonstrate the sensitivity of polymethine dyes to solvent-induced symmetry breaking, confirming the general framework developed for describing their one- and two-photon absorption properties [19, 21, 22, 24].

3.3. Mixtures of CNT and dye

Single-wall CNTs exhibit strong absorption within the ultraviolet, visible, and near-infrared spectral ranges. Two main groups of transitions are observed: E_{11} (or S_{11}), corresponding to the lowest allowed transition of semiconducting CNTs; E_{22} (or S_{22}), corresponding to the second allowed transition of semiconducting CNTs. The position and width of these peaks provide information on the diameter distribution of CNTs; therefore, they allow identification of CNT chirality. Fig. 5a presents a typical PLE map of individually isolated semiconducting CNTs. The PLE map reveals chirality present in the solution, such as (6,5), (7,5), (8,4), (7,3), (8,3), and (7,6), with the main contributions from (6,5), (7,5), (8,4) isolated tubes [11, 12].

Fig. 5b demonstrates absorption spectra for mixtures of the PD-0844 dye with CNTs together with the spectra of neat dispersions of CNT and the neat solution of the dye (all in NMP). Notably, the spectra of neat CNTs (Fig. 5b, curve *2*) and the mixture of fresh dye

solutions with CNTs (Fig. 5b, curve *3*) are very similar in shape, showing no significant differences. This indicates that CNTs do not interact with the PD-0844 molecules in freshly prepared solutions. Furthermore, the absorption spectrum of the mixture for a 9-day-aged solution of the dye and CNTs evidences substantial spectral change with pronounced absorption bands at 1008 and 1160 nm, corresponding to (6,5) and (8,4) chiralities, respectively

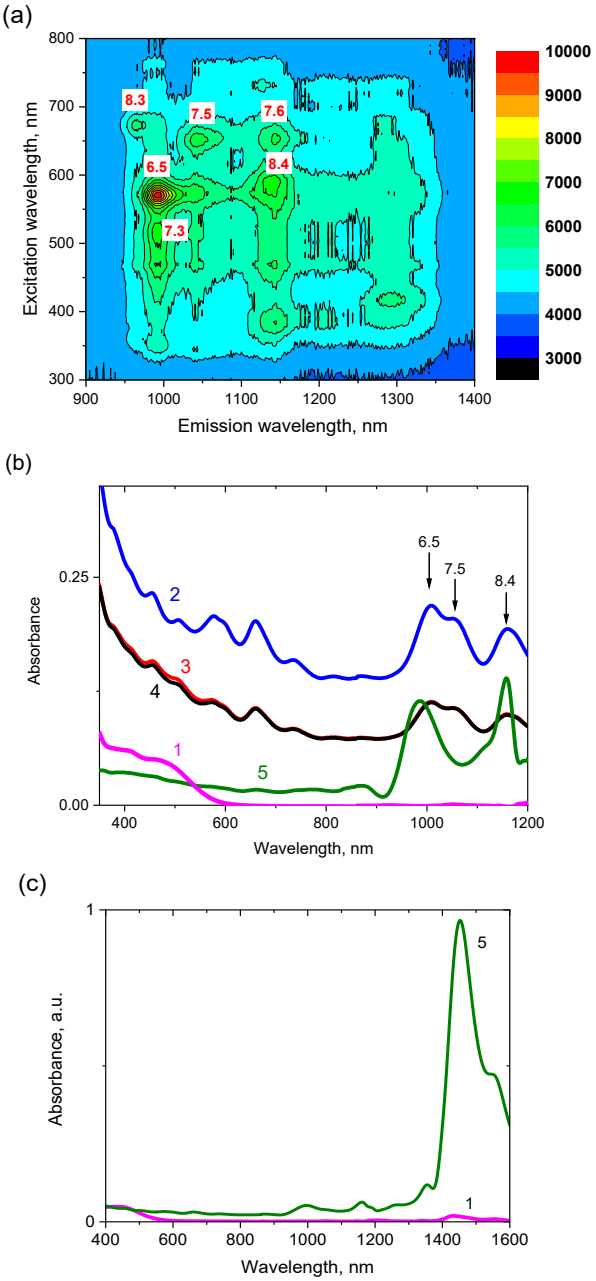

Fig. 5. (a) PLE map of CNT dispersions in NMP. (b, c) Absorbance spectra of 9-day-aged solution of PD-0844 dye (*1*), CNT dispersion (*2*), mixture of fresh solution of PD-0844 dye and CNT (measured immediately after mixing) (*3*), mixture of fresh solution of PD-0844 dye and CNT (measured after 3 days since mixing) (*4*), and mixture of 9-day-aged solution of PD-0844 dye and CNT (*5*); all in NMP solvent. The dye concentration is 0.02 mg/mL.

(Fig. 5b, curve *5*). The absorption band at 1050 nm, corresponding to chirality (7,5), disappears in the spectrum of such aged-dye mixture. Such spectral changes can be associated with selective interaction for CNTs of various chiralities. The nanotubes of (6,5) and (8,4) chiralities interact with the dye by slightly increased absorption of their E_{11} transitions, whereas CNTs with (7,5) chirality interact with the dye and most likely get removed from the dispersion (by aggregation and precipitate formation).

In strongly polar solvents such as NMP, self-assembly of PD-0844 is kinetically restricted, but long-term aging (more than a week) induces weak, red-shifted absorption bands in the range of 1400…1600 nm (Fig. 5c, curve *1*), being indicative of initial aggregation. The presence of CNTs dramatically enhances these bands (Fig. 5c, curve *5*), implying that the CNT surface facilitates the growth of the aggregates into larger supramolecular structures. Further aging of the dye–CNT mixture leads to a substantial increase in aggregate-associated absorption, consistent with progressive assembly on the nanotube surface.

Fig. 6 shows the PLE maps within the visible spectral range for fresh PD-0844 dye solution (Fig. 6a) and a mixture of fresh dye with CNTs (Fig. 6b) in NMP. The PLE maps demonstrate that excitation close to 450…500 nm (from the S_2 state) induces a very intense PL band at 630…640 nm (being previously associated with "dark state" PL). The addition of CNTs does not significantly alter the spectral profile of this emission for a fresh solution of the dye. Aging solutions of the dye quench the PL band at 630 nm in both neat dye and the dye–CNTs mixtures (Figs. 6c, 6d). At the same time, mixtures of the aged solution with CNTs exhibit new "dark" PL bands at 570 and 680 nm, which are absent in fresh solutions. These bands are strongly associated with the presence of CNTs and the interaction of dye molecules in aged solution with the nanotube surfaces. These observations can be rationalized by non-covalent dye-CNT interactions [11, 12]. Non-covalent interactions, such as π–π stacking between the conjugated dye and the graphene-like sidewalls of CNTs, van der Waals forces, and possible hydrogen bonding, promote planar adsorption of dye molecules onto the CNT surface. This interaction might stabilize the symmetric conformation of PD-0844 and modify its excited-state relaxation pathways. This way, the interactions influence the distribution between asymmetrical and symmetrical dye conformations, as reflected in the relative intensities of the 850 and 905 nm PL bands (Figs. 6e, 6f).

The influence of aging of the solution occurs in the following way. Immediately after dissolution, the dye molecules are generally symmetric. Polar solvents shift the equilibrium toward an asymmetric state, and, in the absence of CNTs, aggregation of the dye proceeds very slowly (~10 days). The introduction of CNTs significantly accelerates dye aggregation, which most likely occurs on the CNT surface. Upon adsorption onto the CNT sidewalls, the dye molecules can adopt relatively planar conformations close to the symmetric form, whereas molecules

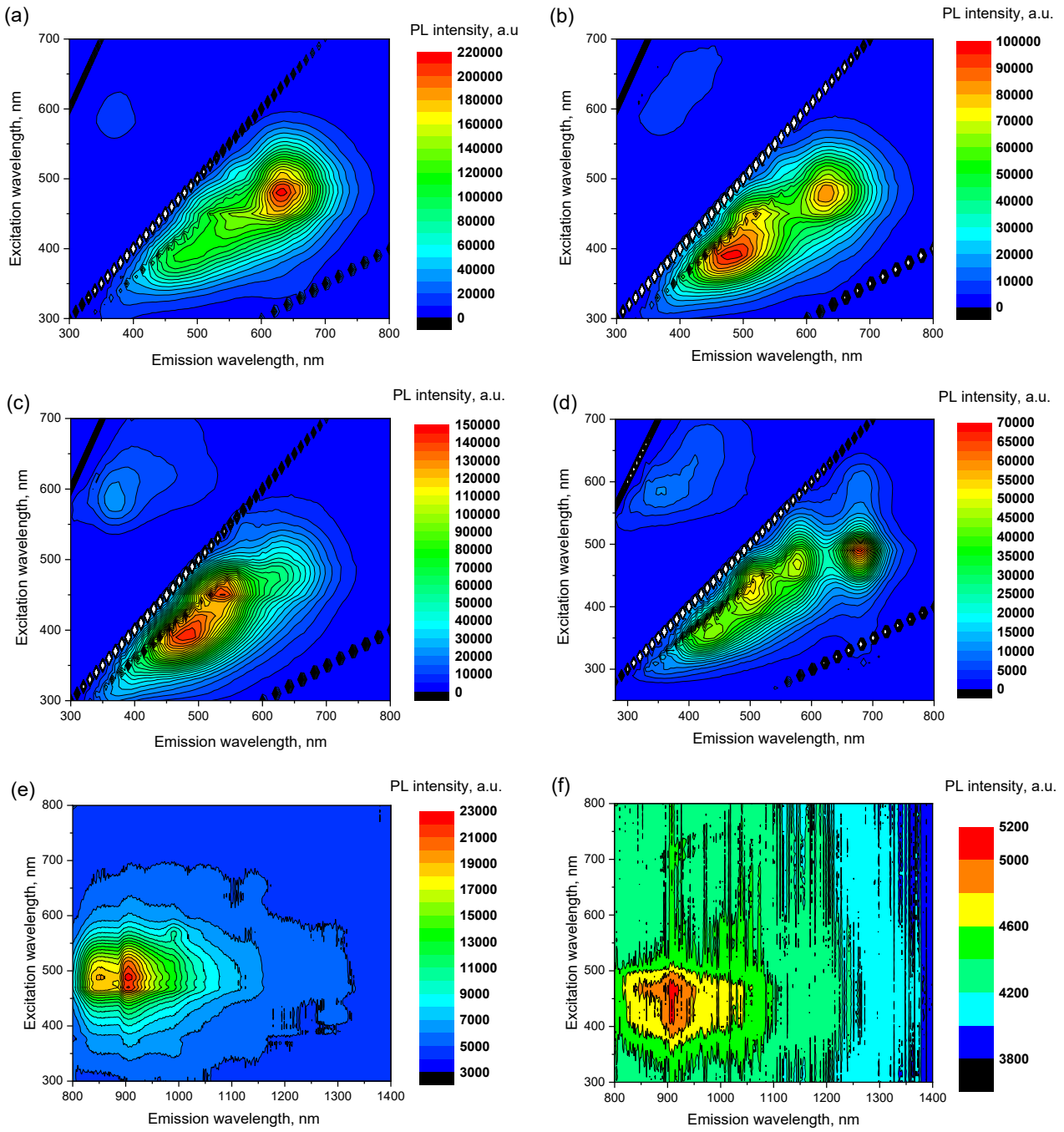

Fig. 6. PLE maps within the visible range for fresh solution of PD-0844 dye (a), mixture of fresh solution of PD-0844 dye with CNT (b), 9-day-aged solution of PD-0844 dye (c), and mixture of 9-day-aged solution of PD-0844 dye with CNTs in NMP (d); PLE maps within the near-IR range for mixtures of fresh (e) and 9-day-aged (f) solution of PD-0844 dye with CNTs; all in NMP. The dye concentration is 0.02 mg/mL.

located away from the CNTs remain predominantly asymmetric. As a result, both conformations coexist in polar solvents. Notably, the dyes show preferential binding to CNTs with (6,5) and (8,4) chiralities, suggesting selective interactions with specific sidewall geometries. Excitation of the dye–CNT system occurs primarily *via* higher electronic states ($S_0 \rightarrow S_n$, $n > 1$), demonstrating anti-Kasha behavior in the visible spectral range.

In addition, formation of new interaction-induced states between the dye and CNTs can provide a rationalization for the emergence of new "dark" PL states at 570 and 680 nm in mixtures with an aged dye solution. Specifically, the weak 680 nm emission in neat dye solution becomes enhanced upon CNTs addition, while the 570 nm band appears only in mixtures of the aged solutions, indicating that CNTs presence is critical for

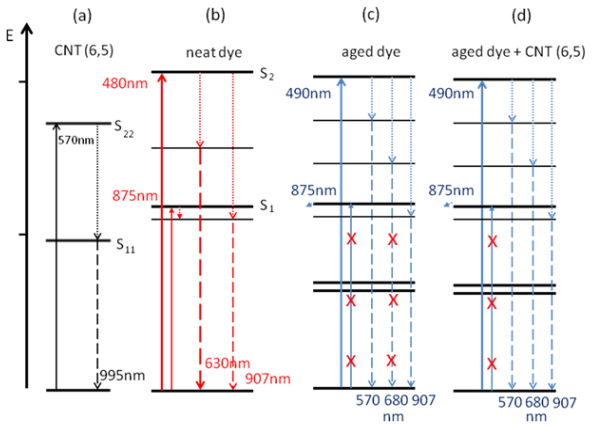

Fig. 7. Energy state diagram and electronic transitions of CNT (a), neat dye (b), aged dye (c), and aged dye – CNTs mixture (d) in NMP solvent. Solid arrows correspond to absorbance, dashed arrows represent emission, dotted arrows show non-radiative transitions, and crossed arrow transitions (at 875 and 680 nm) represent forbidden transitions. CNT of (6,5) chirality is shown as a modelling example, and the diagram for other relevant charities interacting with indotetracarbocyanine dyes can be applied.

formation of these interaction-induced states. Thus, fresh solutions (neat or with CNTs) exhibit "dark" PL at 630 nm, consistent with radiative relaxation following $S_0 \rightarrow S_2$ excitation [24]. Aged solutions in the presence of CNTs have this state quenched and replaced by new interaction-mediated "dark" PL bands at 570 and 680 nm, reflecting the combined effects of the dye conformational stabilization.

Fig. 7 summarizes the spectroscopic states and electronic transitions observed in CNTs, dye, and dye–CNTs mixtures. Fig. 7a represents the transitions for CNTs of (6,5) chirality. Figs. 7b, 7c illustrates the transitions of neat and aged indotetracarbocyanine dyes, including the absorption at 875 nm, which appears only at high dye concentrations and immediately after solution preparation (fresh solution). Fig. 7d shows the spectra of aged dye–CNT mixtures, dominated by strong absorption of aggregated dye molecules and absorption band near 875 nm indicating the presence of symmetric conformations of indotetracarbocyanine molecules adsorbed on the CNT sidewalls. These findings are also in agreement with recent results emphasizing the key roles of symmetry breaking, charge-transfer interactions, and dark-state dynamics in dye photophysics [23].

Observed anti-Kasha PL not only confirms the unusual photophysics of indotetracarbocyanines but also provides a sensitive probe for molecular interactions. Mixtures of such dyes with CNTs constitute a versatile system to study both intrinsic dye properties and solid-state interactions within the dye–CNTs complex, where aggregation is shown to play a decisive role in complex formation. These findings highlight the interplay between molecular organization, aggregation, and excited-state dynamics, offering new avenues for the design of functional dye–nanomaterial systems.

4. Conclusions

A comparative analysis of the optical properties of indotetracarbocyanine dyes in solvents of varying polarity demonstrates that the photophysical behavior of these molecules is governed by a subtle interplay between molecular symmetry, solute–solvent interactions, and dye aggregation effects. The dyes adopt symmetric or asymmetric conformations depending on solvent polarity, aging time, and interaction with CNTs. The observed solvent- and time-dependent spectral evolution is consistent with the ground-state model, which describes the transition from symmetric to asymmetric conformations in polymethine systems. Immediately after dissolving, neat dye molecules reside in the symmetric state; polar solvents gradually shift the conformation toward asymmetry. Even in polar media, aggregation of dye molecules is slow, typically requiring ~10 days. Dye aggregation occurring in the aged solution helps to initiate further coupling of these aggregates with CNTs. The presence of CNTs facilitates rapid aggregation, occurring at the CNT surface. Dye molecules adsorbed on CNT sidewalls may retain a planar symmetric conformation, while molecules in the surrounding solvent adopt asymmetric structures. Consequently, both conformations can coexist in polar solvents.

Overall, these results highlight the subtle sensitivity of indotetracarbocyanine photophysics to solvent environment, molecular conformation, aggregation state, and CNT interactions. The results provide a framework for controlling dye optical behavior through solvent choice, aging, and nanostructure-assisted assembly, with potential implications for optoelectronic applications and energy-transfer systems.

Acknowledgement

A. Verbitsky, Yu. Piryatinski and O. Yatsun acknowledge funding from the National Academy of Sciences of Ukraine (project 1.4B/209).

References

1. Bach G., Daehne S. Cyanine Dyes and Related Compounds, in: *ROOD'S Chemistry of Carbon Compounds*, 2nd suppl. to 2nd ed. Vol. IVB (Heterocyclic Compounds). Ed. M. Sainsbury. Elsevier Science, Amsterdam, 1997. P. 383–481.
2. Yuan J., Yang H., Huang W. *et al.* Design strategies and applications of cyanine dyes in phototherapy. *Chem. Soc. Rev.* 2025. **54**. P. 341. https://doi.org/10.1039/D3CS00585B.
3. Gao Y., Zhu L., Du Z. *et al.* Recent advances in near-infrared cyanine dye-based fluorescent nanoprobes for tumor imaging and therapy. *Int. J. Nanomedicine*. 2025. **20**. P. 13911–13937. https://doi.org/10.2147/IJN.S542880.
4. Piryatinski Y., Verbitsky A., Malynovskyi M. *et al.* Impact of terminal group on temperature-dependent excited state relaxation in cationic dyes. *Chem. Phys.* 2025. **592**. P. 112620. https://doi.org/10.1016/j.chemphys.2025.112620.

5. Sorokin O.V., Bespalova I.I., Yefimova S.L. Fluorescence properties of cyanine dyes molecular aggregates in nanostructured media: A review. *Funct. Mater*. 2025. **32**. P. 323–347. https://doi.org/10.15407/fm32.03.323.
6. Pascal S., Haefele A., Monnereau C. *et al.* On the versatility of electronic structures in polymethine dyes. *Proc. SPIE*. 2014. **9253**. P. 9253A. https://doi.org/10.1117/12.2072624.
7. Masunov A.E., Anderson D., Freidzon A.Ya., Bagaturyants A.A. Symmetry-breaking in cationic polymethine dyes: Part 2. Shape of electronic absorption bands explained by the thermal fluctuations of the solvent reaction field. *J. Phys. Chem. A*. 2015. **119**, No 26. P. 6807–6815. https://doi.org/10.1021/acs.jpca.5b03877.
8. Reimers J.R., Hush N.S. Hole, electron and energy transfer through bridged systems. VIII. Soliton molecular switching in symmetry-broken Brooker (polymethinecyanine) cations. *Chem. Phys.* 1993. **176**. P. 407–420. https://doi.org/10.1016/0301-0104(93)80250-D.
9. Marcelo G.A., Galhano J., Oliveira E. Applications of cyanine-nanoparticle systems in science: Health and environmental perspectives. *Dyes Pigm*. 2023. **208**. P. 110756. https://doi.org/10.1016/j.dyepig.2022.110756.
10. Prousis K.C., Canton-Vitoria R., Pagona G. *et al.* New cationic heptamethinecyanine-graphene hybrid materials. *Dyes Pigm*. 2020. **175**. P. 108047. https://doi.org/10.1016/j.dyepig.2019.108047.
11. Al Araimi M., Lutsyk P., Verbitsky A. *et al.* A dioxaborine cyanine dye as a photoluminescence probe for sensing carbon nanotubes. *Beilstein J. Nanotechnol*. 2016. **7**. P. 1991–1999. https://doi.org/10.3762/bjnano.7.190.
12. Lutsyk P., Piryatinski Y.P., Shandura M. *et al.* Self-assembly for two types of J-aggregates: cis-isomers of dye on the carbon nanotube surface and free aggregates of dye trans-isomers. *J. Phys. Chem. C*. 2019. **123**. P. 19903–19911. https://doi.org/10.1021/acs.jpcc.9b03341.
13. Avouris P., Freitag M., Perebeinos V. Carbon-nanotube photonics and optoelectronics. *Nat. Photonics*. 2008. **2**. P. 341–350. https://doi.org/10.1038/nphoton.2008.94.
14. Hughes K., Iyer K.A., Bird R.E. *et al.* Review of carbon nanotube research and development: Materials and emerging applications. *ACS Appl. Nano Mater.* 2024. **7**, No 16. P. 18695–18713. https://doi.org/10.1021/acsanm.4c02721.
15. Frisch M.J., Trucks G.W., Schlegel H.B. *et al. Gaussian 16, Revision B.01*. Gaussian, Inc., Wallingford, 2016.
16. Toffoli D., Quarin M., Fronzoni G., Stener M. Accurate vertical excitation energies of BODIPY/Aza-BODIPY derivatives from excited-state mean-field calculations. *J. Phys. Chem. A*. 2022. **126**. P. 7137–7146. https://doi.org/10.1021/acs.jpca.2c04473.
17. Limacher P., Mikkelsen K., Lüthi H. On the accurate calculation of polarizabilities and second hyperpolarizabilities of polyacetylene oligomer chains using the CAM-B3LYP density functional. *J. Chem. Phys*. 2009. **130**, No 19. P. 194114. https://doi.org/10.1063/1.3139023.
18. Fu J., Padilha L.A., Hagan D.J. *et al.* Molecular structure – two-photon absorption property relations in polymethine dyes. *J. Opt. Soc. Am. B*. 2007. **24**. P. 56–66. https://doi.org/10.1364/JOSAB.24.000056.
10. Terenziani F., Painelli A., Katan C. *et al.* Charge instability in quadrupolar chromophores: Symmetry breaking and solvatochromism. *J. Am. Chem. Soc*. 2006. **128**. P. 15742–15755. https://doi.org/10.1021/ja064521j.
20. Davydov A.S. *Theory of Molecular Excitons*. Springer, 2013.
21. Terenziani F., Przhonska O.V., Webster S. *et al.* Essential-state model for polymethine dyes: Symmetry breaking and optical spectra. *J. Phys. Chem. Lett*. 2010. **1**. P. 1800–1804. https://doi.org/10.1021/jz100430x.
22. Pascal S., David S., Andraud C., Maury O. Near-infrared dyes for two-photon absorption in the short-wavelength infrared: strategies towards optical power limiting. *Chem. Soc. Rev*. 2021. **50**. P. 6613–6658. https://doi.org/10.1039/D0CS01221A.
23. Eskandari M., Roldao J.C., Cerezo J. *et al.* Counterion-mediated crossing of the cyanine limit in crystals and fluid solution: Bond length alternation and spectral broadening unveiled by quantum chemistry. *J. Am. Chem. Soc*. 2020. **142**, No 6. P. 2835–2843. https://doi.org/10.1021/jacs.9b10686.
24. Malpicci D., Lucenti E., Giannini C. *et al.* Prompt and long-lived anti-Kasha emission from organic dyes. *Molecules*. 2021. **26**. P. 6999. https://doi.org/10.3390/molecules26226999.

Authors and CV

A.B. Verbitsky, PhD, Head of the Dep. of Molecular Electronics, Institute of Physics. Authored over 100 publications. His current research interests include the investigation of electronic properties of low-dimensional structures and nanocomposites. E-mail: avsky123@gmail.com, https://orcid.org/0000-0002-8680-3570

Yu.P. Piryatinski, PhD, Leading Scientific Researcher, Institute of Physics. Authored over 250 publications. Expertise: electronic and excitonic processes in nanostructured molecular crystals, photoluminescent time-resolved spectroscopy of nano-structured and low-dimensional organic and inorganic materials. E-mail: yuri.piryatinski@gmail.com, https://orcid.org/0000-0001-7225-8084

O.D. Kachkovskyy 1946 – 2026 Doctor of Chemical Sciences, Senior Researcher at the V.P. Kukhar Institute of Bioorganic Chemistry and Petrochemistry. Authored over 300 publications. His research interests were biochemistry, quantum chemical calculations, linear conjugated systems.
https://orcid.org/0000-0002-8418-9079

O.V. Yatsun, PhD, Lecturer at the National University of Life Resources and Environmental Management of Ukraine. Authored over 10 publications. His research interests are spectroscopic investigations of low-dimensional molecular objects with a fine focus on dye molecular aggregates. E-mail: yatsun.o@nubip.edu.ua, https://orcid.org/0009-0003-6415-1174

K.O. Maiko, Assistant of the Department of Medical Radiophysics at the Faculty of Radio Physics, Electronics and Computer Systems, Taras Shevchenko National University of Kyiv. Authored over 10 publications. Her research interests include quantum chemical calculations, molecular docking, biophysics. https://orcid.org/0000-0002-2035-1284, e-mail: maiko_kate@ukr.net

A.G. Rozhin, PhD, Reader at Aston University (Birmingham, UK). Authored over 200 publications. His current research interests span: nanomaterials synthesis by laser ablation and chemical routes; nanomaterials surface functionalization for photonic, biomedical diagnostic and drug delivery applications; optical spectroscopy of advanced materials.
E-mail: A.ROZHIN@aston.ac.uk,
https://orcid.org/0000-0003-2271-8227

P.M. Lutsyk, PhD, Senior Lecturer at Aston University (Birmingham, UK). Authored over 50 publications. The areas of his expertise include materials science: characterization of organic, nano- and bio-materials, polymers, dyes, nanocomposites, hybrid 'organic-inorganic' systems; spectroscopy: photoluminescence emission & excitation maps, time-resolved photoluminescence, absorption, reflectance, Raman, photovoltage & photocurrent. https://orcid.org/0000-0002-7004-1946

Authors' contributions

Verbitsky A.B.: methodology, validation, investigation, writing – review & editing.
Piryatinski Yu.P.: key ideas, conceptualization, data analysis, validation, supervision.
Kachkovskyy O.D.: investigation, quantum-chemical calculations, formal analysis, supervision
Yatsun O.V.: investigations, literature analysis, writing & editing.
Maiko K.O.: data curation, validation, quantum-chemical calculations.
Rozhin A.G.: conceptualization, formal and data analysis, supervision.
Lutsyk P.M.: key ideas, conceptualization, supervision, writing – original draft, writing – review and editing.

Регульоване випромінювання індотетракарбоціанінових барвників внаслідок варіації сольватів та взаємодії з вуглецевими нанотрубками

А.Б. Вербицький, Ю.П. Пірятинський, О.Д. Качковський, О.В. Яцун, К.О. Майко, А.Г. Рожин, П.М. Луцик

Анотація. Індотетракарбоціаніни належать до родини довгих ціанінових барвників, які легко змінюють форму молекули від симетричного ціаніноподібного до асиметричного поліенового стану. На конформацію таких молекул, а отже, і на їх фотолюмінесцентне випромінювання може впливати безліч факторів. У цій статті ми досліджували фотофізичну поведінку індотетракарбоціанінових барвників у різних розчинниках та в сумішах з одностінними вуглецевими нанотрубками. Результати виявили залежні від концентрації, старіння та полярності розчинника спектральні особливості таких барвників, що дозволило встановити ключові механізми зміни випромінювання. Спектральні зміни були пов'язані із залежними від симетрії молекулярними конформаціями індотетракарбоціанінів, а також із їхньою здатністю взаємодіяти з поверхнею вуглецевих нанотрубок. Нові смуги випромінювання виникають у спектрах фотолюмінесценції внаслідок взаємодії барвник–нанотрубка, що визначається π–π стекінгом та електростатичними ефектами. Така поведінка узгоджується з викликаною адсорбцією агрегацією барвника на поверхні нанотрубки та з утворенням нових фотоіндукованих станів випромінювання.

Ключові слова: ціанінові барвники, вуглецеві нанотрубки, фотолюмінесценція, флуоресценція, ціанінові та поліенові стани, старіння розчину.